Journal of Engineering
journal homepage: www.joe.uobaghdad.edu.iq
Number 6 Volume 26 June 2020

Mechanical and Energy Engineering

Thermal Modeling of Solar Still Coupled with Heat Pipes and Experimental Validation

Najim A. Kadhum *
Ph.D. student
Ministry of science and technology
Baghdad, Iraq
najim_kadhum@yahoo.com

Prof. Dr. Najm A. Jassim
University of Baghdad, college of engineering
Baghdad, Iraq
Najmosawe@yahoo.com

Dr. Kamal H. Lateef
Chief Researcher
Ministry of science and technology
Baghdad, Iraq
kamalhlatif @yahoo.com

ABSTRACT

Water is the basis of the existence of all kinds of life, so obtaining it with good quality represents a challenge to human existence and development especially in the desert and remote cities because these areas contain small populations and water purification requires great materials and huge amounts of fossil fuels resulting pollution of the environment. Cheap and environmentally friendly desalination methods have been done by using solar distillations.

Passive solar stills have low yields, so in this research, the problem is overcome by connecting four heat pipes which are installed on the parabolic concentrator reflector with passive solar still to increase the temperature of hot water to more than 90°C, as a result, the yield increases. An extensive theory is studied to manufacture two systems: the first consists of passive solar still has dimensions are 1000 mm × 500 mm and the glass cover tilted at the angle 33°. It is approximately equal to the latitude of the city of Baghdad [(Latitude: (33.34° N) Longitude: (44.4° E)]. This gives 5.04 kg/m^2.day, the second solar still which is associated with 4 heat pipes gives a water yield of about 7. 2 kg/m^2.day. This means that the improvement in the daily production of distilled water is 50 % over the productivity of the passive solar still All results above are calculated when the depth of water is 1. 5 cm. In addition, heat balance for each part of the system is achieved and calculations of the performance of the solar still are done by using the program in the language of Matlab. All these results are compared with the experimental ones of different depths of water (1.5 cm, 2 cm, 3 cm, and 4 cm) which are taken from the experimental part to ensure the system reliability at different weather conditions in Baghdad throughout the year and to give a good approach. The system associated with heat pipes gives promising results and can be widely used for its abundant productivity and durability of its components. (TDS) and (pH) value are carried out in the laboratory and it is found that water is safe and pure for drinking.

Keywords: solar still, desalination, heat pipes.

*Corresponding author

Peer review under the responsibility of University of Baghdad.
https://doi.org/10.31026/j.eng.2020.06.14

2520-3339 © 2019 University of Baghdad. Production and hosting by Journal of Engineering.
This is an open access article under the CC BY4 license http://creativecommons.org/licenses/by /4.0/).

Article received: 16/7/2019
Article accepted: 9/9/2019
Article published:1/6 /2020

نمذجة رياضية لمقطر شمسي مقترن مع انابيب حرارية وتحقق تجريبي

نجم عبد كاظم
طالب دكتوراة
وزارة العلوم والتكنولوجيا

نجم عبد جاسم
استاذ
قسم الهندسة الميكانيكية/ جامعة بغداد

كمال حسين لطيف
رئيس مهندسين
وزارة العلوم والتكنولوجيا

الخلاصة

الماء اساس وجود الحياة بكل انواعها لذلك فان الحصول عليه بنوعية جيدة يمثل تحدي للوجود البشري والتطور خاصة في المناطق الصحراوية والبعيدة عن المدن لان هذه المناطق تحتوي تجمعات سكانية صغيرة وان تصفية الماء تحتاج امكانات مادية كبيرة وكميات هائلة من الوقود الاحفوري ينتج عنها تلوث البيئة.وبسبب ذلك تم البحث عن طرق تصفية رخيصة وصديقة للبيئة باستخدام المقطرات الشمسية.

المقطرات الشائعة انتاجيتها منخفضة ، لذا تم في هذا البحث التغلب على هذه المشكلة عن طريق ربط اربعة انابيب حرارية مثبتة على عاكس بشكل قطع مكافي مع المقطر الشائع لزيادة درجة حرارة الماء إلى أكثر من 90°C، ونتيجة لذلك تزداد الانتاجية للمقطر.

تمت دراسة نظرية لتصنيع منظومتين الاولى مكونة من مقطر شمسي شائع ابعاده 1000 mm × 500 mm والغطاء الزجاجي مائل بزاوية 33° تقريبا ويساوي خط العرض لمدينة بغداد (خط عرض 33.34°= N و خط طول 44. 4° = L) وأعطى انتاجية 5.04 $kg/m^2.day$ والثانية مقطر شمسي مقترن مع اربعة انابيب حرارية وأعطى كمية ماء بحدود 7. 2 $kg/m^2.day$ وهذا يعني أن التحسن في الإنتاج اليومي للمياه المقطرة كان % 50 اعلى من إنتاجية المقطر الشمسي الشائع. وجميع النتائج اعلاه تم حسابها عندما يكون الماء على عمق 1.5 cm وفي الجزء النظري تم حساب معاملات انتقال الحرارة داخل وخارج المقطر وإجراء موازنة حرارية لكل جزء من اجزاء المنظومة وحساب اداء المنظومة من خلال برنامج بلغة ماتلاب وقورنت مع النتائج العملية لأعماق ماء مختلفة (1.5 cm ,2 cm, 3 cm, 4 cm) ولظروف جوية مختلفة في بغداد وعلى مدار السنة وأعطت مقاربة جيدة مع نتائج عملية تم اخذها من الجزء العملي للتاكد من موثوقية المنظومة. وان المنظومة المقترنة من الانابيب الحرارية اعطت نتائج واعدة ويمكن الاستفادة منها على نطاق واسع لوفرة انتاجيتها.ومتانة مكوناتها وتمت دراسة كمية الاملاح المذابة (TDS) والاس الهيدروجيني (pH) في المختبر وتبيّن أن الماء صالح للشرب.

الكلمات الرئيسية: المقطر الشمسي, التصفية, الانابيب الحرارية.

1. INTRODUCTION

The crisis of processed water represents the greatest challenge concerned with growth and development in the world. For example, although water covers two - thirds of the planet, drinking water is less than 1%. (**Sampath, et al., 2013**). The rested water, is snow or groundwater that may be close to the surface of the earth or deep groundwater which is far from the surface of the earth, is difficult to reach or extract and it is very expensive too. As a result, many methods must be developed to obtain potable water such as reverse osmosis, multistage flash distillation and thin-film distillation, but these methods are expensive in terms of the high cost of the station. The used tools and fuel cause several major hazards including pollution.

The use of renewable energy method is the main idea of this research to benefit from the solar radiation which is coming from the sun for water purification that considerably abundant to solve the problem of drinking water in Iraq.

(**Masoud, et al., 2010**), studied theoretically of solar still in the city of Chabahar-Iran. The dimensions of solar still are 2000 mm× 500 mm and the glass cover tilted at the angle 25°. A heat balance of energy equations of solar still is solved under certain minor assumptions. The temperatures of the glass cover, the saline water, and the basin are calculated. The researcher finds that productivity is high in the summer months and it is a function of solar radiation. They find distilled water is approximately 4.81 liters as a daily yield in July and 3.67 liters as a daily yield in December and the efficiency reaches its maximum value in the noon. (**Sampath, et al., 2011**),

studied thermal modeling of single basin solar still. The researcher concluded that can increase the production of water distillation to about 72 % as a result of high temperature due to the coupled flat plate collector with the evacuated tube. (**Kiam Beng Yeo et al 2014**), performs a numerical investigation to study the heat balance of energy equations on a single slope basin solar still to get clean water from brackish water in an enclosed space. Critical parameters have been studied, such as a slope angle of the glass cover, the quantity of water in basin and wind speed. Simulation is carried out on the relation between the slope angle and the latitude of the experimental location. Finally, they find that increasing water in the basin leads to a decrease in water production and that wind speed is one of the factors which increases water production. The result shows that the optimum angle is equal to 10° facing south (latitude angle) and predicts that the productivity of solar still is (2 kg. m^{-2}.day^{-1}). (**Kalbande, et al., 2016**), studied theoretically analysis of solar still integrated with 10 evacuated tubes. The experiment has been achieved in summer; the researcher found that if the basin water depth is 3 cm, distilled water is approximately 8 liters as a daily yield. The maximum daily efficiency is 34.39 %. (**Mehul and Piyush, 2016**), an experiment was carried out on the single slope solar still connected with the evacuated tubes. A mathematical model is also constructed to solve the energy balance equations for the different component of system. Their study displays that the efficiency without evacuated tubes are: 20%, 19%, 15% and efficiency with evacuated tubes are: 41%, 45%, and 35% respect to water depths which are: 1 cm, 2 cm, and 3 cm respectively. The theoretical and experimental comparisons show a good agreement.
(**Hitesh, et al., 2017**), an experimental study has been developed and conducted on single basin solar still. Then, the researchers can increase the production of water distillation as a result of high temperature due to couple with evacuated tubes. On the other hand, the maximum yield of the solar still coupled with heat evacuated tubes is 4.94 kg/m^2.day and the yield of the passive solar still is 2. 5 kg/m^2.day. This means the improvement in the daily production of distilled water was 97.6 % over the productivity of the passive solar still. In the interval from (11-July-2011to 11-June), the result above was taken at depth of water is equal to 3 cm. **(Saad and Mohanad, 2017),** performed an experiment on the solar still coupled with evacuated tube heat pipes. The study is carried out on a single basin solar still in Bagdad city for certain days in many months to investigate the effect of heat pipes on distillate output and efficiency of the system under local climatic conditions. Many different water samples are used in this study: sea water and river water in the basin for different depths of water (1,2 and 3 cm). The study showed that single basin solar still coupled with 10 heat pipes to enhance the productivity from 3.4724 to 7.0375 kg/m2. day**. (Kotebavi et al., 2018),** studied solar still coupled with heat pipes and experimental study has been developed and conducted on three types of still namely: passive solar still, coupled with heat pipes, coupled with evacuated tubes. They could increase the production of water distillation to about 40 % over the productivity of the solar still coupled with evacuated tubes as a result of high temperature due to coupling with heat pipes. (**Mowaffaq and Najim 2019**), an experimental study has been developed and conducted on a single basin solar still in Mosul city (Latitude:35.866°N, Longitude:43.296°E), In the interval from May to August, they could increase the production of water distillation as a result of good insulation by 20.785% and 19.864% when using thermal insulation of 4 and 5 cm respectively. The daily production of distilled water is increased by 14.147 % as water depth changes from 5cm to 4 cm. While the present work is divided into two sections:
The theoretical investigation involves a numerical study of thermal modeling which is carried out on two types of solar stills which are: passive solar still and solar still coupled with 4 heat pipes. The energy balance equations are solved by Matlab program for each component of solar still with several critical factors including reflectivity, transmissivity, the angle of the glass cover, climate

condition (ambient temperature, the intensity of the solar radiation, water depth). The present theoretical work covers water depths: (1.5 cm, 2 cm, 3 cm, and 4 cm).
The experimental investigation includes a set of experiments carried out on two types of solar still to study the factors affecting on the performance and the efficiency of the solar still by changing the depth of water in the basin liner which are the same water depth used in the theoretical part of this study under various outdoor climatic conditions related to the two types of solar stills.

2. MATH EMATICAL MODELS

The mathematical model is done by using equations of energy balance for all parts of the solar still and heat pipes.

2.1 Assumptions

Many assumptions are carried out to simplify the mathematical model for the case under study. Therefore, the following assumptions are used in the modeling:
1- The level of water inside the basin is constant.
2- The system is under quasi steady-state.
3- There are no temperature gradients in all components of solar still.
4- The water vapor is an ideal gas.
5- The system is tight so that no vapor leakage occurs outside.

2.2 Governing Equations

. Modes of heat transfer occurring in each component of solar still as shown in Fig. 1 and according to the assumptions listed in the previous article, the governing equations are follow (**Tiwari et al., 2007**):

:

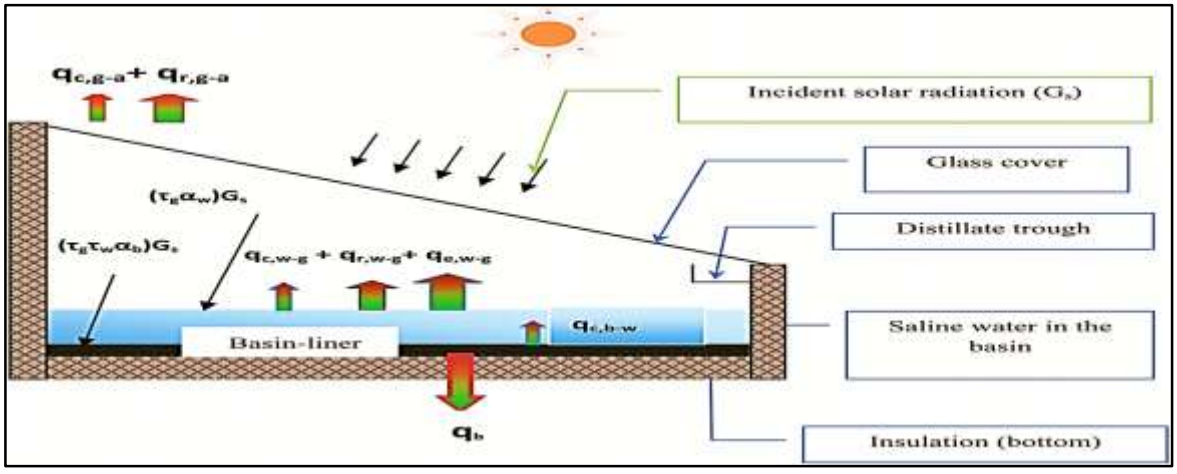

Figure 1. Heat transfer modes in solar still.

2.2.1 Energy Balance of Glass Cover in Passive Solar Still.

$$Q_{gc,in} = Q_{gc,out} \quad (1)$$

$$m_{gc}CP_{,gc}\frac{dT_{gc}}{dt} = A_{gc}F_{gc}G_{g,ef} + A_w h_{t,w-gc}\left(T_w - T_{gc}\right) - A_{gc}h_{c,gc-a}\left(T_{gc} - T_a\right) - A_{gc}h_{r,gc-sk}\left(T_{gc} - T_{sk}\right) \quad (2)$$

2.2.2 Energy Balance of Basin Liner in Passive Solar Still.
The energy balance of basin Liner is given by:

$$Q_{b,in} = Q_{b,out} \quad (3)$$

$$m_b CP_b \frac{dT_b}{dt} = A_w\left[F_b G_{g,ef} - h_{c,b-w}(T_b - T_w) - U_{bo}(T_b - T_a)\right] \quad (4)$$

$$U_{bo} = \frac{k_{ins}}{X_{ins}} \quad (5)$$

2.2.3 Energy Balance of Water Mass in Passive Solar Still.

$$Q_{w,in} - Q_{w,out} = \frac{dE_w}{dt} \quad (6)$$

$$m_w CP_{,w} \frac{dT_w}{dt} = A_w\left[F_w G_{g,ef} + h_{c,b-w}(T_b - T_w)\right] - \dot{m}_d L H_w - A_w h_w\left(T_w - T_{gc}\right) - A_s U_{sw}(T_w - T_a) \quad (7)$$

2.2.4 Useful Heat Gained by Heated Pipes.

The heat pipes give a useful energy to the given water as follows (**Dimir et al., 2008**):

$$Q_u = F_R \times A_{ET} \times \left[(\propto \tau)_C I_t - U_{LC} \frac{A_L}{A_{ET}} (T_w - T_a)\right] \quad (8)$$

Where:
$F_R = 0.831$, $U_{LC} = 2.44\, W/m\,.C°$, $(\propto \tau)_C = 0.8$,
A_{ET} = Total length of the tube × diameter of absorber glass = 0.44 m^2
$A_L = \pi\, A_{ET} = 1.39 m^2$

2.2.5 Energy Balance of Water Mass in Solar Still Coupled with Heated Pipes.

$$Q_{w,in} - Q_{w,out} = \frac{dE_w}{dt} \quad (9)$$

$$m_w CP_{,w} \frac{dT_w}{dt} = A_w\left[F_w G_{g,ef} + h_{c,b-w}(T_b - T_w)\right] + Q_u - \dot{m}_d L H_w - A_w h_w\left(T_w - T_{gc}\right) - A_s U_{sw}(T_w - T_a) \quad (10)$$

2.3 Internal Heat Transfer.
In the solar still heat is transferred internally in the system by convection, conduction and radiation.

2.3.1 Convective Heat Transfer Rate.
The heat flux transferred from water to glass cover by free convection is calculated according to the law (**Velmurugan, et al., 2007):**

$$q_{c,w-gc} = h_{c,w-gc}\,(T_w - T_{gc}) \quad (11)$$

2.3.2 Convective Heat Transfer Coefficient.
Many models have been designed and developed to find convective heat transfer coefficient between the water and the glass cover. One of these methods is developed by (**Dunkel, 1969)**:

$$h_{c,w-gc} = 0.884\left[\left(T_w - T_{gc}\right) + \frac{T_w\left(P_w - P_{gc}\right)}{268.9 \times 10^3 - P_w}\right]^{1/3} \quad (12)$$

Where:

$P_w = \exp(25.317 - \frac{5144}{T_w})$

$P_{gc} = \exp\left(25.317 - \frac{5144}{T_{gc}}\right)$

(**Tiwari, et al., 2005**), give the convective heat transfer coefficient between the basin liner and the saline water which is:

$h_{c,b-w} = \frac{K_W}{X_W} C(Gr \times Pr)^n$ (13)

Where:

$C = 0.54$ and $n = \frac{1}{4}$

$Pr = \frac{\mu \times CP}{K}$, $Gr = \frac{g \times \beta \times \Delta T \times \rho^2 \times L_c}{\mu^2}$, $Ra = Gr \times \Pr$

2. 3.3 Evaporative Heat Transfer Coefficient.

Due to solar radiation, water gets heated and the evaporative heat transfer coefficient from water to glass can be expressed in the form (**Dunkle, 1969**):

$h_{e,w-gc} = 0.016273\, h_{c,w-gc} \left[\frac{(P_w - P_{gc})}{(T_w - T_{gc})}\right]$ (14)

2.3.4 Evaporative Heat Transfer Rate.

The evaporative heat transfer rate between glass and water is calculated according to the relation (**Velmurugan, et al**., **2007**):

$q_{e,w-gc} = h_{e,w-gc}\,(T_w - T_{gc})$ (15)

2.3.5 Radiative Heat Transfer Rate.

Radiation heat flux transfer from water to glass cover is calculated according to the following equation (**Tiwari, et al., 2005**):

$q_{r,w-gc} = \varepsilon_{eff}\, F_{1-2}\, \sigma\left(T_w^4 - T_{gc}^4\right)$ (16)

Where:

$\varepsilon_{eff} = (\frac{1}{\varepsilon_{gc}} + \frac{1}{\varepsilon_w} - 1)^{-1}$, $\varepsilon_g = \varepsilon_w = 0.9$

2.3.6 Radiative Heat Transfer Coefficient.

Radiative heat transfer coefficient from water to glass cover is given by (**Dunkel, 1969)**:

$h_{r,w-gc} = \varepsilon_{eff}\, \sigma(T_w^2 + T_{gc}^2)\left(T_w + T_{gc}\right)$ (17)

The total heat transfer from water to glass is given by,

$q_{t,w-gc} = q_{c,w-gc} + q_{e,w-gc} + q_{r,w-gc}$ (18)

The total heat transfer coefficient from water to glass is given by,

$h_{t,w-gc} = h_{e,w-gc} + h_{c,w-gc} + h_{r,w-gc}$ (19)

2.4 External Heat Transfer

2.4.1 Top Loss Heat Transfer Coefficient.

Heat losses from the outer surfaces of the glass cover to the atmospheric are got by convection and radiation. Thus the losses of the upper surface are given by (**Dunkel, 1969)**:

$q_{t,gc-a} = q_{c,gc-a} + q_{r,gc-a}$ (20)

2.4.2 Radiative Heat Transfer Coefficient.
Radiative heat transfer coefficient from glass cover to atmospheric is given by (**Badran, 2007**):

$$h_{r,gc-a} = \varepsilon_{gc}\sigma\left[\frac{(T_{gc}^4 - T_{sk}^4)}{(T_{gc} - T_a)}\right] \quad (21)$$

$$T_{sk} = T_a - 6 \quad (22)$$

2.4.3 Radiative heat transfer rate.
Radiative heat transfer rate from glass cover to atmospheric is given by (**Tiwari, et al., 2005**):

$$q_{r,gc-a} = h_{r,gc-a}\,(T_{gc} - T_{sk}) \quad (23)$$

2.4.4 Convective Heat Transfer Coefficient.
Convective heat transfer coefficient from glass cover to atmospheric is given by (**Tiwari, et al., 2005**):

$$h_{c,gc-a} = 2.8 + 3 \times V_w \quad (24)$$

2.4.5 Convective Heat Transfer Rate.
Convective heat transfer rate from glass cover to atmospheric is given by (**Tiwari, et al., 2005**):

$$q_{c,gc-a} = h_{c,gc-a}\,(T_{gc} - T_a) \quad (25)$$

2.5 Distillate Yield.
2.5.1 The Hourly Distillate Yield of Still
The hourly distillate yield of solar still can be found from the correlation listed below (**Sampath Kumar, 2011**):

$$\mathrm{m}_{ew} = \frac{q_{e,w-gc}}{LH_w} \times 3600 \times A_w = \frac{h_{e,w-gc}\,(T_w - T_{gc})}{LH_w} \times 3600 \times A_w \quad (26)$$

When the temperature is greater than $70°C$, the latent heat of evaporation is given in the following relation (**Sampath Kumar, 2011**):

$$LH_w = 3.1615 \times 10^6[1 - 7.6160 \times 10^{-4} \times T_w] \quad (27)$$

And when the temperature is below $70°C$, the latent heat of evaporation is given in the following relationship:

$$LH_w = 2.4935 \times 10^6[1 - 9.4779 \times 10^{-4} \times T_w + 1.3132 \times 10^{-7} \times T_w^2 - 4.7974 \times 10^{-9} \times T_w^3] \quad (28)$$

2.5.2 Daily Distillate Output of the Still.
Daily distillate output from solar still is given as follow:

$$\mathrm{M_{ew}} = \sum_{j=1}^{24} \mathrm{m}_{ew(j)} \quad (29)$$

j = Hours of day.

2.6 Efficiency of the Solar Still
Instantaneous energy efficiency is given by the following relationship (**Radwn, et al., 2009**):

$$\eta_{energy} = \frac{\mathrm{m}_{ew} \times LH_w}{I_t \times A_w \times 3600} * 100\% \quad (30)$$

3. NUMERICAL SOLUTIONS
3.1 Numerical Solution Procedure for Passive Solar Still
The system of nonlinear transient equations is solved implicitly to find the system of linear algebraic equations for the p^{th} time step

3.1.1. Glass Cover (gc)

The energy balance equations (2) for the glass cover of solar still are formulated as follows:

$$T_{gc}^{p} = C_{10} + C_{11} T_{gc}^{p-1} + C_{12} T_{w}^{p} \quad (31)$$

Where:

$$C_{10} = \frac{\Delta t\,(A_{gc} F_{gc} G_{g,ef} + A_{gc} h_{c,gc-a} T_a + A_{gc} h_{r,gc-sk} T_{sk})}{\Delta t\,(A_w h_{gc} A_{gc} h_{c,gc-a} + A_{gc} h_{r,gc-sk}) + m_{gc} CP_{gc})}$$

$$C_{11} = \frac{m_{gc} CP_{gc}}{\Delta t\,(A_w h_{gc} A_{gc} h_{c,gc-a} + A_{gc} h_{r,gc-sk}) + m_{gc} CP_{gc})}$$

$$C_{12} = \frac{\Delta t\, A_w h_{t,w-gc}}{\Delta t\,(A_w h_{gc} A_{gc} h_{c,gc-a} + A_{gc} h_{r,gc-sk}) + m_{gc} CP_{gc})}$$

3.1.2 Basin Liner (b)

The energy balance equations (4) for the basin liner of solar still are formulated as follows:

$$T_{b}^{p} = C_{20} + C_{21} T_{b}^{p-1} + C_{22} T_{w}^{p} \quad (32)$$

Where:

$$C_{20} = \frac{\Delta t\, A_w (\, F_b G_{g,ef} + U_{bo} T_a)}{\Delta t\, A_w (h_{c,b-w} + U_{bo}) + m_b\, CP_b}$$

$$C_{21} = \frac{m_b\, CP_b}{\Delta t\, A_w (h_{c,b-w} + U_{bo}) + m_b\, CP_b}$$

$$C_{22} = \frac{\Delta t A_w h_{c,b-w}}{\Delta t\, A_w (h_{c,b-w} + U_{bo}) + m_b\, CP_b}$$

3.1.3 Water in Basin (w)

The energy balance equation (7) for the water mass of solar still is formulated as follows:

$$T_w = C_{30} + C_{31}\, T_w^{p-1} + C_{32}\, T_{gc}^{p} + C_{33}\, T_b^{p} \quad (33)$$

Where:

$$C_{30} = \frac{\Delta t(A_w F_w G_{g,ef} + A_s U_{Sw} T_a)}{\Delta t\, A_w (h_{c,b-w} + h_w) + \Delta t\, A_s U_{sw} + m_w\, CP_w)}$$

$$C_{31} = \frac{m_w\, CP_w}{\Delta t\, A_w (h_{c,b-w} + h_w) + \Delta t\, A_s U_{sw} + m_w\, CP_w)}$$

$$C_{32} = \frac{\Delta t A_w h_w}{\Delta t\, A_w (h_{c,b-w} + h_w) + \Delta t\, A_s U_{sw} + m_w\, CP_w)}$$

$$C_{33} = \frac{\Delta t A_w h_{c,b-w}}{\Delta t A_w (h_{c,b-w} + h_w) + \Delta t\, A_s U_{sw} + m_w\, CP_w)}$$

3.2 Numerical Solution Procedure for Solar Still Coupled with Heat Pipes

The same method is used to derive the temperature equations of the glass cover and the basin that is applied in passive solar still but the equations of water temperature are changed because of the

heat that is added from the heat pipes (Q_u). The energy balance equation (10) for the solar still coupled with heat pipes is formulated as follows:

$$T_w = C_{40} + C_{41}\, T_w^{p-1} + C_{42}\, \mathrm{T}_{gc}^{p} + C_{43}\, T_b^{p} \quad (34)$$

Where:

$$\mathrm{C}_{40} = \frac{\Delta \mathrm{t}(\mathrm{A}_w\, \mathrm{F}_w \mathrm{G}_{g,ef} - \dot{m}_d L H_w + A_s U_{Sw}\, \mathrm{T}_a + F_R \times U_{LC}\, \frac{A_L}{A_{ET}} + F_R \times (\propto \tau)_C I_t)}{\Delta \mathrm{t}\, \mathrm{A}_w (h_{c,b-w} + h_w) + \Delta \mathrm{t}\, A_s U_{sw} + m_w\, CP_w + \Delta \mathrm{t}\, F_R \times U_{LC}\, \frac{A_L}{A_{ET}})}$$

$$\mathrm{C}_{41} = \frac{m_w\, CP_w}{\Delta \mathrm{t}\, \mathrm{A}_w (h_{c,b-w} + h_w) + \Delta \mathrm{t}\, A_s U_{sw} + m_w\, CP_w + \Delta \mathrm{t}\, F_R \times U_{LC}\, \frac{A_L}{A_{ET}})}$$

$$\mathrm{C}_{42} = \frac{\Delta \mathrm{t} \mathrm{A}_w h_w}{\Delta \mathrm{t}\, \mathrm{A}_w (h_{c,b-w} + h_w) + \Delta \mathrm{t} A_s U_{sw} + m_w\, CP_w + \Delta \mathrm{t}\, F_R \times U_{LC}\, \frac{A_L}{A_{ET}})}$$

$$\mathrm{C}_{43} = \frac{\Delta \mathrm{t}\, \mathrm{A}_w h_{c,b-w}}{\Delta \mathrm{t}\, \mathrm{A}_w (h_{c,b-w} + h_w) + \Delta \mathrm{t}\, A_s U_{sw} + m_w\, CP_w + \Delta \mathrm{t}\, F_R \times U_{LC}\, \frac{A_L}{A_{ET}})}$$

A computer program is written in MATLAB (version 10.0) to solve the system of equations. See **Table 1** for Reference design and operational parameters for the solar still.

Table 1. Reference design and operational parameters for the solar still.

glass cover	basin liner	saline water	isolation
$A_{gc} = 0.64m^2$	$A_b = 0.5m^2$	$A_w = 0.5m^2$	$X_{ps} = 0.05\ m$
$m_{gc} = 6.25kg$	$m_b = 18.453kg$	$m_w = 7.5 - 20kg$	$X_{pw} = 0.011\ m$
$\alpha_{gc} = 0.127$	$\alpha_b = 0.95$	$\alpha_w = 0.05$	$K_{pw} = 0.12\, W/m.k$
$K_{gc} = 1.05\, W/m.k$	$K_b = 47.6\, W/m.k$	$\tau_w = 0.95$	$K_{ps} = 0.034\, W/m.k$
$Cp_{gc} = 750 J/kg.k$	$Cp_b = 477 J/kg.k$	$Cp_w = 4190 J/kg.k$	$X_{pw} = 0.011\ m$
$X_{gc} = 0.004\ m$	$X_b = 0.001\ m$	$X_w = 1.5, 2\ , 3, 4\ cm$	$X_{ps} = 0.05\ m$
$\tau_{gc} = 0.78$		$\rho_w = 0.02$	

Various physical properties are used in presented work are calculated from **(ASHREA 2001)**

3.3 Variations of Biot Numbers for Solar Still Components

The variations of Biot number are within the acceptable limit ($Bi \leq 0.1$) for using the lumped capacitance method.

4. EXPERIMENTAL SETUP

An experimental rig which is designed, developed and constructed is shown in **Fig.2** and it is used in the present work to study the solar still. In the present work, different measurements and instruments have been used such as solar meter, anemometer, electronic balance, and digitals data logger thermometers. The components of rig test are described below.

4.1 Basin

The basin is made from galvanized iron with thickness of 1. 5 mm and the basin has an area ($1\ m \times 0.5\ m$) and the height of the back wall is 0.525m while the front wall of 0.20m.

The base of the basin is painted black to absorb the largest amount of heat falling on the basin itself while the side walls of the basin are painted white to reflect the heat on the base of the

basin. Each solar still is equipped with two valves; one is used for supplying water to the basin and the other used for getting rid of the remaining water. It is also used for cleaning basin from the salts and dirty in order to be used again.

Figure 2. A photograph showing the two types of solar still.

4.2 Basin Cover

In this present work, the cover is made from a glass plate whose thickness effects the performance of the solar still. The researchers (**Hitesh and Shah 2011**), used identical glass plates with different thicknesses (4mm, 8mm, and 12mm). They find that the lower glass thickness of 4mm is better because of increasing the evaporative heat transfer coefficients, water temperature, the efficiency of a solar still, convective heat transfer coefficient as well as the distillate water output. Consequently, the thickness which is used in this experiment is 4mm.

The best angle of the glass surface is 10° to ensure that the drop of condensed droplets inside the trough and to ensure that it does not fall back and also affect on the optimal utilization of solar radiation So, normally $\beta = \varphi$ for annual performance (**Abdul Jabbar, 2011**).

Thus the angle of the glass cover is taken as 33.34° and approximately is equal to the latitude of the city of Baghdad $[(\textbf{Latitude}: (33.34^\circ\ N) \textbf{Longitude}: (44.4^\circ\ E)]$ gives maximum yield production which are shown in **Fig. 3**.

4.3 Distillate Trough

A rectangular channel with dimensions $(50\ cm \times 2cm \times 3cm)$ (made of galvanized steel) was installed inside the galvanized iron box, which lies on the lower edge of each condensing surface to collect distilled water.

4.4 Sealant:

Sealants should be used in special conditions such as: remain resilient at very low temperatures, durable, low cost and easily applicable. The materials that are used include tapes silicon, tars, and Putty.

Sealant foam is put between the glass cover and the basin material to absorb the shock and silicone material that fills the gap between them to seal and prevent leakage.

4.5 Insulation

The loss of heat from the sides and bottom of the basin is undesirable because it reduces the performance of the solar still. Therefore, the heat losses should be reduced by the use of good insulators that have low thermal conductivity (K).

In this present work, two-layer insulation is used, the first layer from Polystyrene has a thickness of 5 cm and the second layer of plywood has a thickness of 11mm which are shown in **Fig. 3**.

4.6 Instrumentation

In this research, used measuring devices are calibrated by the Ministry of Science and Technology to take readings of the intensity of solar radiation, wind speed, the mass of water, total dissolved solids (TDS) and pH of water, and temperatures of water, basin, glass cover, and ambient air temperature.

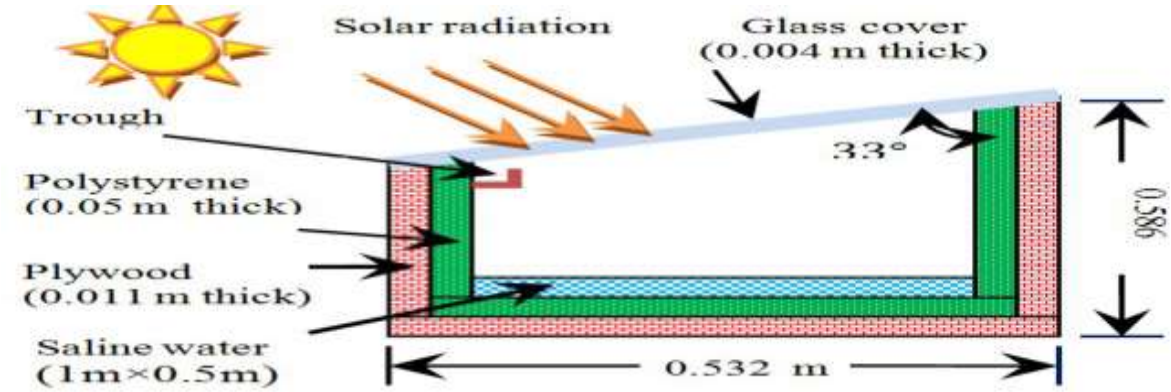

Figure 3. Cross-section through the conventional solar still.

4.7 Heat Pipes

Four heat pipes are used in this work was installed on a parabolic reflector as shown in **Figs. 4** and the specification of heat pipes is listed in **table 2**.

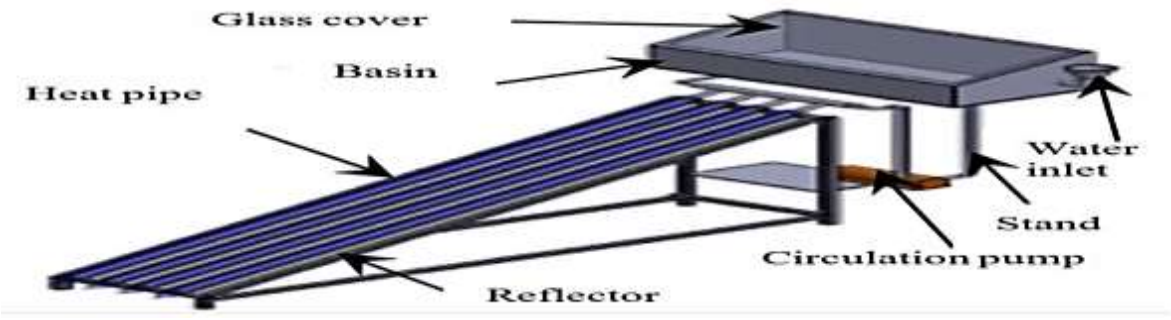

Figure 4. Schematic of solar still coupled with heat pipes.

Table 2. Specifications of heat pipes.

Model No.	**KO-450**
Type	Heat pipe evacuated glass tube solar collector
Dimensions	640 (w) × 2088 (L) × 113(H) mm
Gross area	1.33 m^2
Aperture area	1.09 m^2
Fluid capacity	0.45 lit. (Header section)
Heat pipe working fluid	Fluorocarbon
Number of tubes	4

5. DISCUSSION AND RESULT

The research focuses on the energy analysis of the passive solar still and solar still coupled with heat pipes that are studied in Baghdad city. The temperature of the two types of solar stills, the quantity of produced water, the efficiency of energy, the pressure, the absorptivity and the heat transfer coefficients by evaporative, radiative and convective have been investigated. It is found that the active solar still produces more distilled water per unit area of basin than the conventional solar still.

The theoretical results are compared with the experimental results and gave a good approach. On the other hand, the results are compared with other researchers of the credibility of the results.

5.1 Energy Analysis

5.1.1 Heat Transfer Coefficients

Figs. (5 & 6) show the hourly variation of the theoretical values of heat transfer coefficients from water in the basin to the glass cover (as a result of evaporation, radiation, and evaporation) of passive solar still and solar still coupled with heat pipes respectively. The evaporation heat transfer coefficient increases gradually until it reaches its maximum values which are: (27.85 $W/m^2.°C$ and 41.31 $W/m^2.°C$) at 2 p.m. and then the evaporation heat transfer coefficient of the two types of solar stills mentioned above decrease. The convective and radiative heat transfer coefficients are much smaller than the evaporation heat transfer coefficient. The maximum values of convective heat transfer coefficients are (3.22 $W/m^2.°C$ and 3.52 $W/m^2.°C$) of the two types of solar stills respectively. The corresponding values of radiative heat transfer coefficients are (6.43 $W/m^2.°C$ and 6.98 $W/m^2.°C$) respectively. It is obvious that the patterns of theoretical for heat transfer coefficients are the same.

Fig. 7 shows the hourly variation of the theoretical values of evaporation heat transfer coefficients from water in the basin to the glass cover (as a result of evaporation) of passive solar still and solar still coupled with heat pipes respectively. It is very clear that the evaporation heat transfer coefficients increase with the time and reaches its maximum values of the two types mentioned above at 2 p.m. which are: (27.85 $W/m^2.°C$ and 41.31 $W/m^2.°C$) respectively and then decrease. The values of evaporation heat transfer coefficients of solar still coupled with heat pipes are greater than passive solar still by 48.33%. It is very close to the increment of distillate output.

5.1. 2 Temperature

Figs. (8 & 9) show the hourly variation of the ambient, basin, glass cover and saline water temperatures of passive solar still and solar still coupled with heat pipes respectively, which are recorded according to the simulation program of a typical day (3 – April – 2018) at water depth (2 cm). It is very obvious that the temperatures have the following tendency: temperatures start

initially together and then gradually go up as a result of increasing the intensity of solar radiation until temperatures reach their maximum values after 1 p.m. Then temperatures begin to decrease. In other words, the daylight can be divided into three intervals as follows: In the first interval (from 6 a.m. to 9 a.m.) hourly variation of temperatures is insignificant because of the low intensity of solar radiation while during the second interval (from 9 a.m. to 2 p.m.) is relatively high temperatures variation because the solar radiation is high. In the third interval after 2 p.m., the solar radiation decreases and temperatures decrease too.

It is clear from the figure that the basin temperature is slightly more than saline water due to some physical properties which are: high absorption coefficient, low transmissivity, and high thermal conductivity. On the other hand, the basin of solar still is insulated by two layers which are: plywood and polystyrene to reduce heat loss from system to the environment leading to an increase of basin temperature in addition to the factors mentioned above. The obtained conclusion is that both solar radiation and temperature have the same behavior.

5.2 Efficiency Analysis

Figs. (10 & 11) show the instantaneous energy efficiencies of passive solar still and solar still coupled with heat pipes respectively.

In the passive solar still, see **Fig. 10,** the energy efficiency goes up from (0%) at 8 a.m. and reaches its maximum value is (27%) when its maximum quantity of evaporative heat is (195.64W/m^2) at 2 p.m.

In solar still coupled with heat pipes see **Fig. 11**, the energy efficiency goes up from (0) and reaches its value is (77.86%) when its maximum quantity of evaporative heat is (1152.8W/m^2) at 2 p.m.

5.3 Saturated Water Pressure

Fig. 12 shows the variation of saturated water pressures at glass cover and water temperatures as a function of time. The change of saturated water pressure starts increasing since the early morning hours until it reaches the maximum value after 1 p.m. and then it starts gradually to decrease until it reaches the lowest value in the dark of both cases mentioned above. This means that the saturated water pressure at water temperature starts from 2590 N/m^2 at 7 a. m and reaches its maximum value 10532 N/m^2 after 1 p.m. while saturated water pressure glass temperature starts from 2200 N/m^2 at 7 a.m. and reaches its maximum value 7000 N/m^2 after 1 p.m. As a result, the growth of saturated water pressure is the same trend of growth of solar radiation. It is very clear that the figure shows the same behavior as solar radiation.

5.4 Verification of The Results

5.4.1 Comparison with Present Experimental Work

Figs. (13 & 14) show the variation of theoretical and experimental cumulative distillate production of passive solar still and solar still coupled with heat pipes at the University of Baghdad. It should be noted that these observations conform to the computed levels of effective irradiance. Productivity is estimated from the present theoretical work which is closer to the experimental data. It should also be mentioned that theoretical productivity is more than the experimental one. Passive solar still and solar still coupled with heat pipes overestimate the distillate yield slightly by about 5%, 6% respectively due to vapor and distillate leakage from practical solar still and measurement errors. It is very clear that the hourly distillate output is relatively low of the two solar stills when the level of insolation is low. As a result, it is difficult to measure the distillate yield with higher accuracy. So, the daily distillate outputs are found to be more reliable in all seasons except winter.

5.4.2 Comparison with Previous Theoretical Results

Figs. (15 & 16) show the theoretical comparison between present work and theoretical work achieved by other researchers that the behavior of evaporative heat transfer coefficients of current work during solar distillation is the same as the behavior of (**Dunkle, 1969**), (**Hitesh, 2011**) and (**Medugu, 2009**) and that the difference in values is due to different hypotheses and weather conditions. It is shown by comparison that the behavior of heat transfer coefficients of current work during solar distillation is the same as the behavior of (**Dunkle, 1969**), (**Hitesh Panchal, 2011**) and that the difference in evaporative heat transfer coefficients and convective heat transfer coefficients is due to different hypotheses and weather conditions.

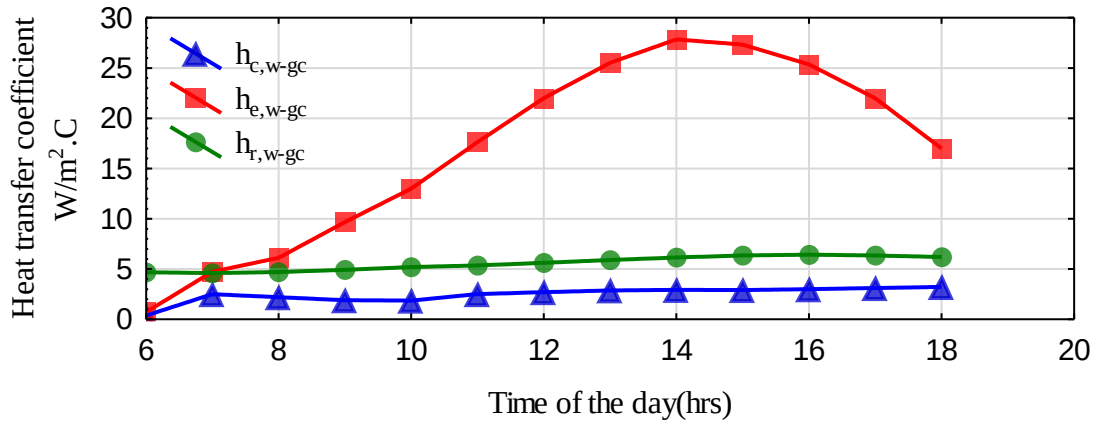

Figure 5. Hourly variation of heat transfer coefficients (evaporative, convective and radiative) of passive solar still as a function of time at depth of water (2cm) (3-April -2018)

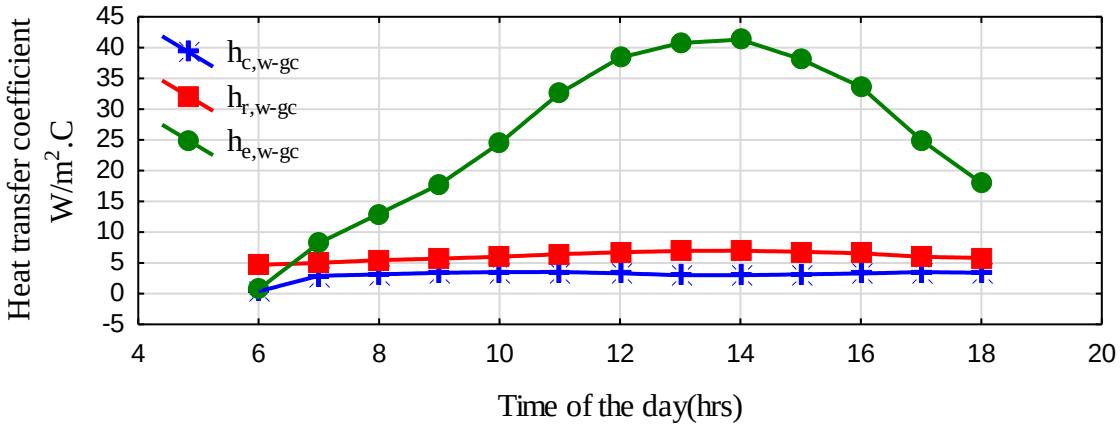

Figure 6. Hourly variation of heat transfer coefficients (evaporative, convective and radiative) of solar still coupled with heat pipes as a function of time at depth of water (2cm) (3-April -2018)

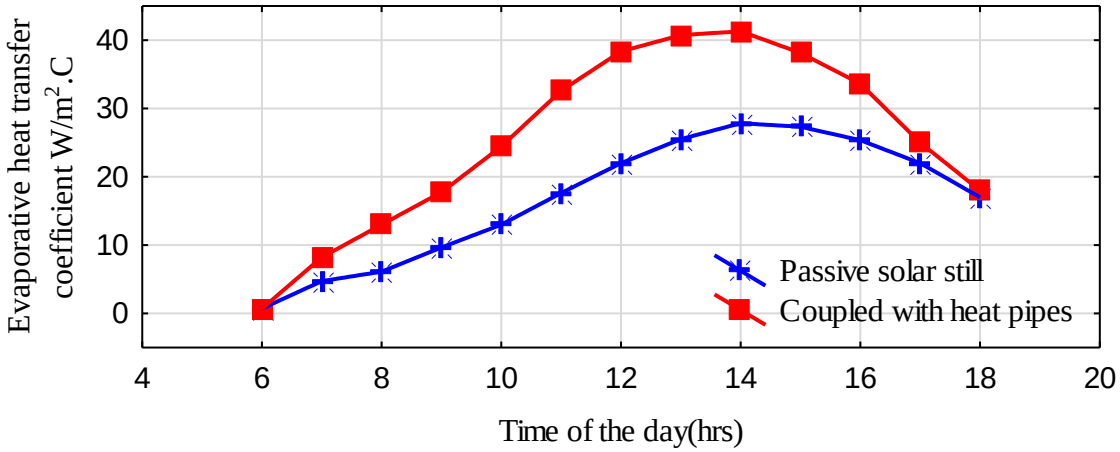

Figure 7. Hourly variation of evaporative heat transfer coefficients of two types of solar still at depth of water (2cm) (3-April -2018)

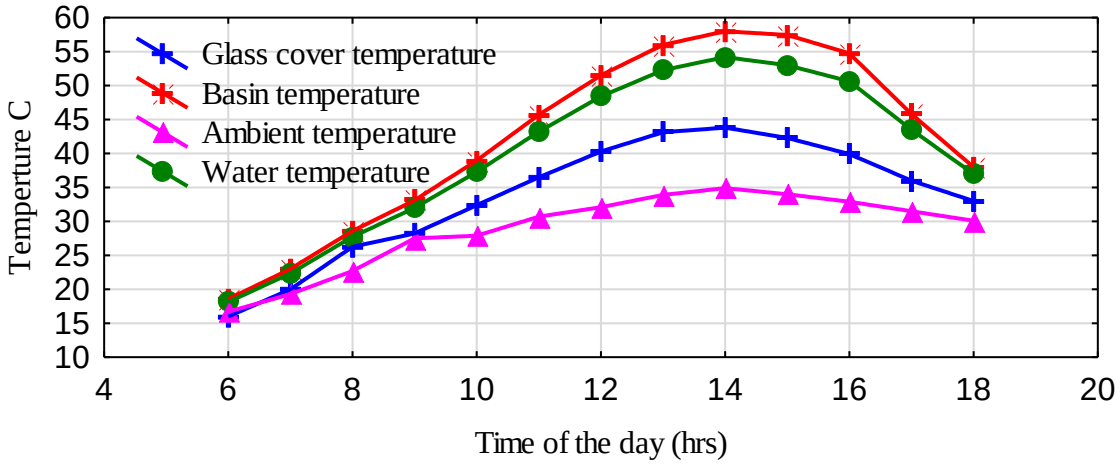

Figure 8. hourly variation of basin, water, glass cover tempertures for passive solar still from 6A.M to 6P.M (3-April-2018)

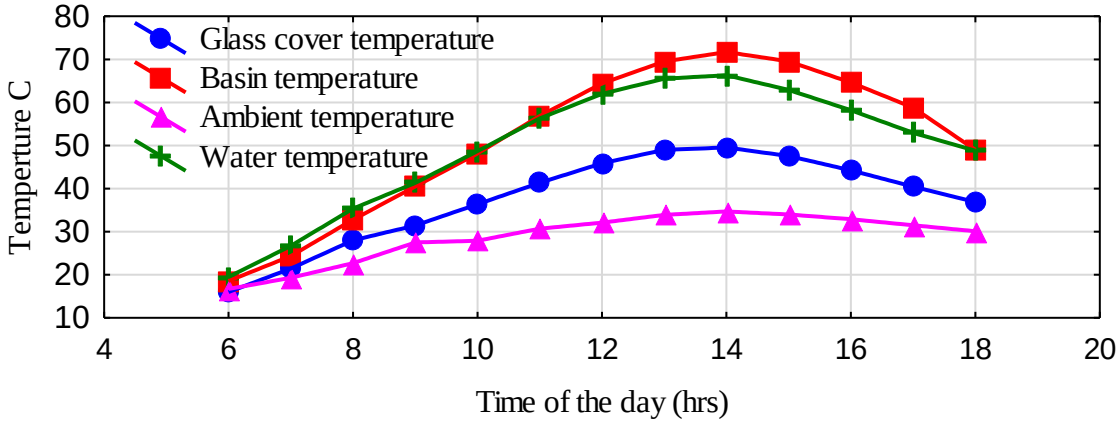

Figure 9. Hourly variation of basin, water, glass cover and ambient temperatues of solar still coupled with heat pipes at depth of water (2cm) (3-April -2018)

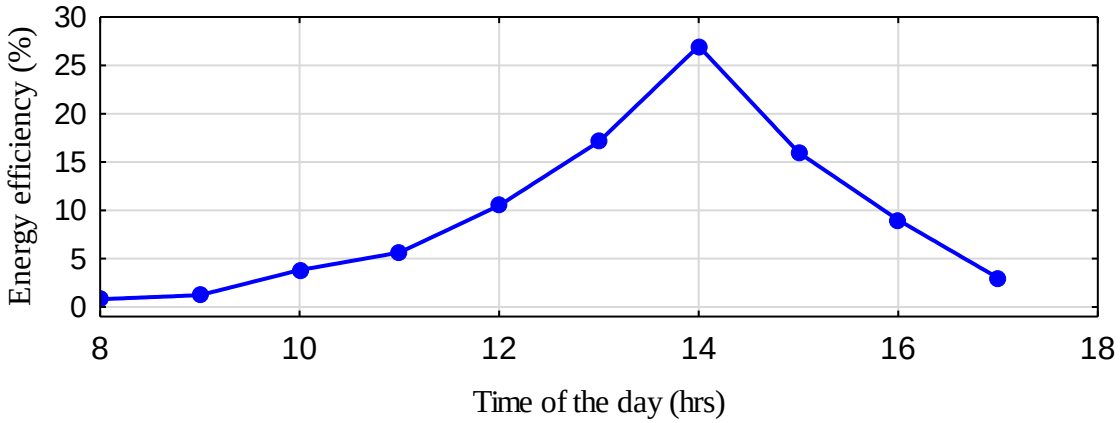

Figure 10. Hourly variation of overall instantenous energy efficiency for passive solar still from 8A.M to 5P.M at depth of water (2cm)
(3-April-2018)

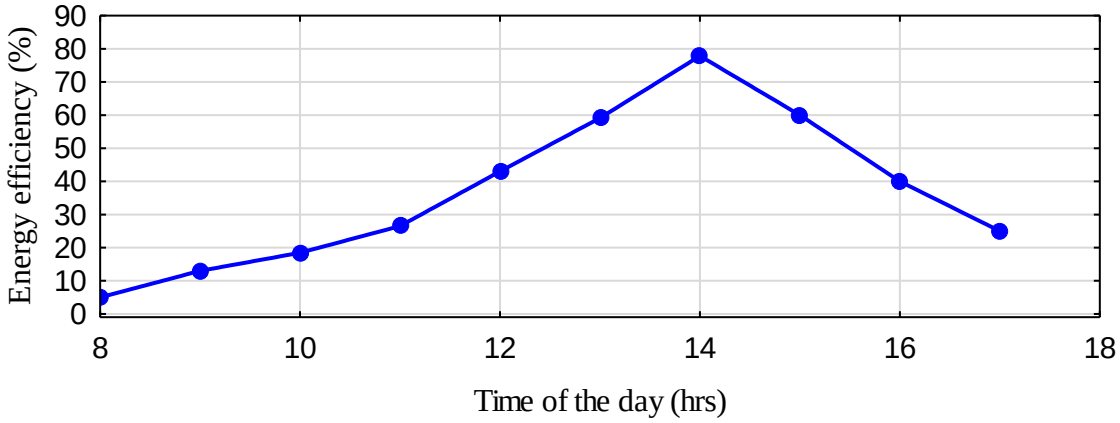

Figure 11. Hourly variation in overall instantenous energy efficiency for solar still coupled with heat pipes from 8A.M to 5P.M at depth of water (2cm)
(3-April-2018)

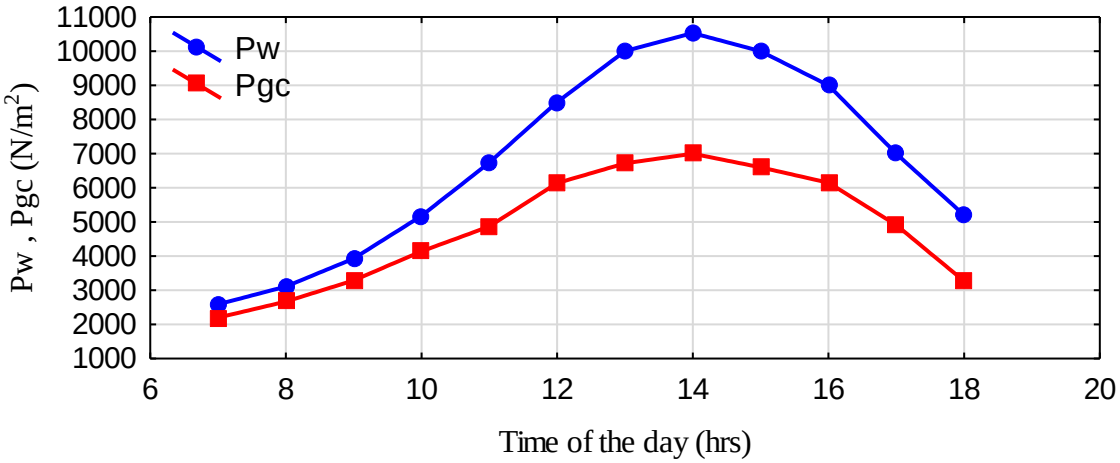

Figure 12. Hourly variation saturated watre pressures at glass cover and water temperature at depth of water (1.5 cm) (27-March.-2018)

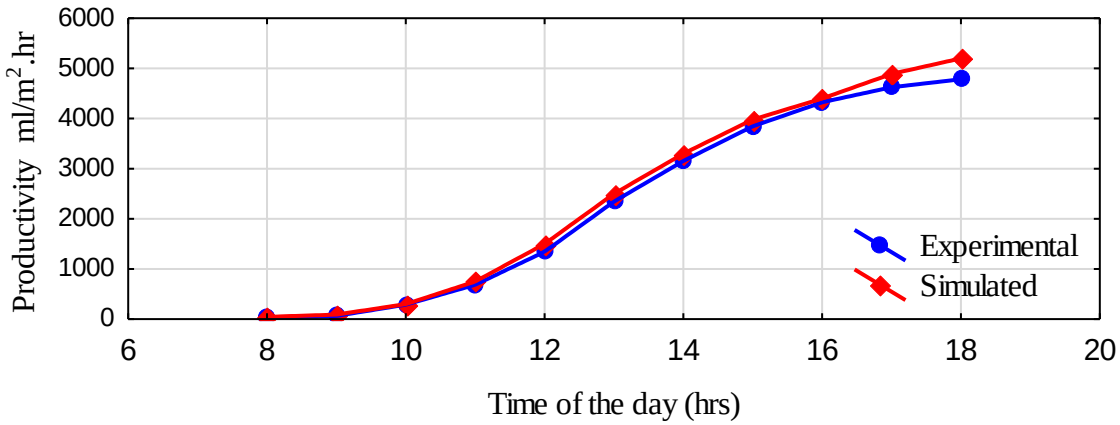

Figure 13. Comparison between theoretical and experimental cumulative productivity for passive solar still at depth of water (1.5 cm) (15-May -2018)

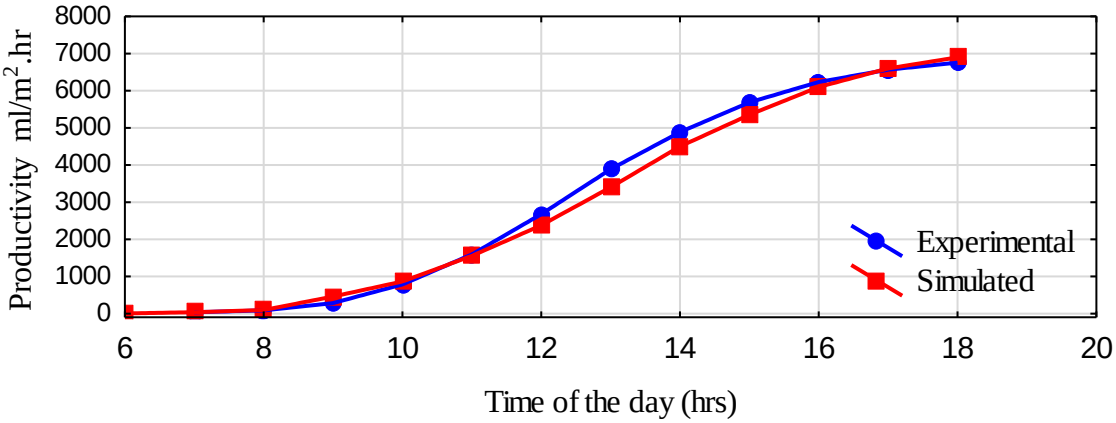

Figure 14. Comparison between theoretical and experimental cumulative productivity for solar still coupled with heat pipes at depth of water (1.5 cm) (15-May -2018)

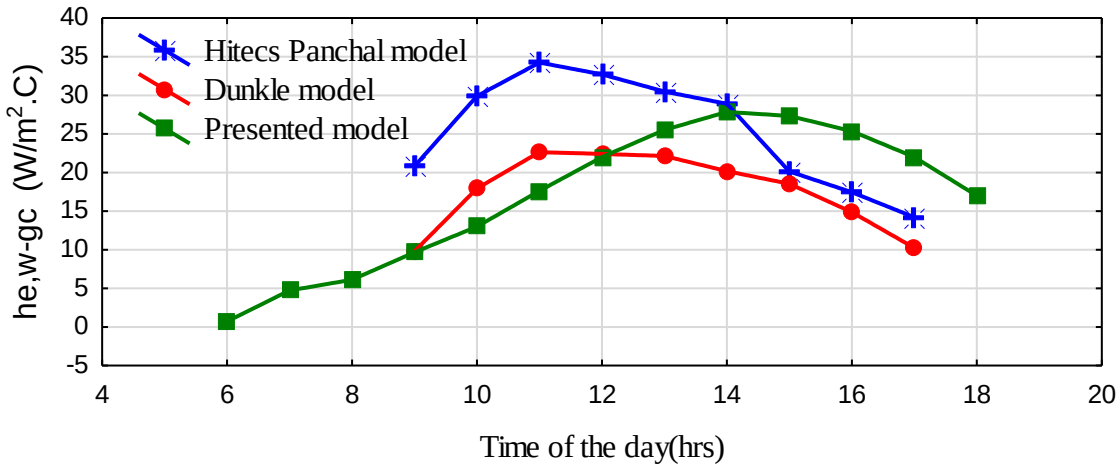

Figure 15. Variation of evaporative heat transfer coefficients of passive solar still as a function of time at at depth of water (2cm) (24-January -2018)

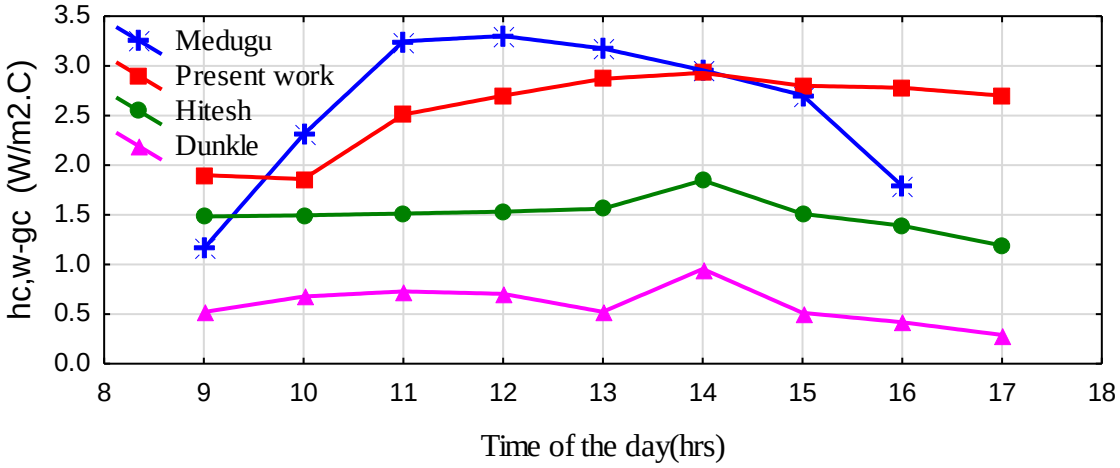

Figure 16. : Variation of convective heat transfer coefficients of passive solar still as a function of time at depth of water (2cm) (24-January -2018)

6. CONCLUSIONS

Theoretical and experimental investigations of the passive solar still and solar still coupled with heat pipes under Baghdad, climate conditions have been performed in the present work. The following conclusions have been drawn from the present investigation:

1-The highest productivity obtained for each system are as follows: 4.8 liters in the passive solar still and 7.2 liters in the solar still coupled with heat pipes because increasing the rate of heat transfers to water coming from heat pipes.

2-The output of the solar still coupled with the heat pipes installed above the reflector increases approximately by 50% due to more solar radiation which is absorbed by the heat pipes.

3– The distillate of water decreases in months (June, July, and August) because of the high temperature of the glass. As a result, it decreases the difference temperature between the glass cover and saline water.

4-The depth of the water affects on distillation productivity. In all experiments, it is found that increasing the depth of water reduces distillate productivity because increasing the mass of water in the basin needs to absorb a large amount of heat to raise its temperature and then delays the process of evaporation and condensation.

5- Future work recommendations can be given in the following points: studying the effect of the number of heat pipes and the effect of changing the angles in different seasons. In addition to that, selection of the optimum angles that are used to maximize the productivity of solar still and studying the effect of phase change material on the yield of solar still.

7. REFERENCES

- Abdul Jabbar N. Kalipha, 2011, On the effect of cover tilt angle of the simple solar still on its productivity in different season and latitudes, Energy Conversion and management 52, pp.431-436.
- ASHRAE, 2001, ASHRAE Handbook Fundamentals, SI ed. Atlanta: American Society of Heating, Refrigerating and Air-Conditioning Engineers.
- Dimri, V., Sarkar B., Sing, U.and Tiwari G.N., 2008, Effect of condensing cover material on yield of an active solar still: an experimental validation, Desalinationpp,178, 189.
- Dunkle R.V., 1969, Solar water distillation – the roof type still and multiple effect diffusion still, Heat Transfer, Conference, Part V, International Developments in Heat Transfer, University of Colorado, pp. 895.
- Hitesh N. Panchal and Shah P. K., 2011, Effect of Varying Glass cover thickness on Performance of Solar still: in a Winter Climate Conditions, International Journal of Renewable Energy Research, Vol.1, No.4, pp.212-223.
- Hitesh Panchala, Ravishankar Sathyamurthyb, Pandeyc A. K., Mahesh Kumard, T. Arunkumare and Patela D. K., 2017, International Journal of Ambient Energy"https://doi.org/10.1080/01430750.2017.1378720
- Kalbande S. R.,.Khampalkar V.P, Priyankanayak and Sneha D.Deshmukh, 2016, Development and evaluation solar still integrated with evacuated tubes", IMPACT, International Journal of Research in Applied, Natural and Social Sciences Vol. 4, Issue 12, pp. 99-106.
- Kiam Beng Yeo, Cheah Meng Ong and Kenneth Tze Kin Teo, 2014, Heat Transfer Energy Balance Model of Single Slope Solar Still, Journal of Applied Sciences, 14: pp. 3344-3348.
- Kotebavi, V., Pramod, B.V.N., Prudhvi Raj, J., Hari, Krishnan, S.S.,2018, Performance analysis of a solar still coupled with evacuated heat pipes (Conference Paper) (Open Access) IOP Conference Series: Materials Science and Engineering Volume 310, Issue 1.
- Masoud Afrand, Amin Behzadmehr and Arash Karimipour, 2010, A Numerical Simulation of Solar Distillation for Installation in Chabahar-Iran, World Academy of Science, Engineering and Technology International Journal of Mechanical and Mechatronics Engineering Vol:4, No:11.
- Medugu D. W. and Ndatuwong L. G., 2009, Theoretical analysis of water distillation using solar still, International Journal of Physical Sciences Vol. 4 (11), pp. 705-712, November.
- Mehul Agrawal and Piyush Nema, 2016, Experimental works on Solar distil combined to EGT (Evacuated Glass Tube) By means of an air as unimportant Fluid, International Journal of Engineering Development and Research, Vol. 4, Issue 4.

- Mowaffaq Ali Hammadi, Najim Abid Jasim, 2019, Experimental Study of Solar Still Under Influence of Various Conditions, Iraq, Journal of Engineering, Vol. 25, no.2, pp.57- 71.
- Omar O. Badran, Mazen M Abu-Khader, 2007, Evaluating thermal performance of a single slope solar still: Heat and Mass Transfer, 43:985–95
- Radwn S.M., Hassanain A.A. and Abu Zeid M.A., 2009, Single Slope Solar Still for Sea Water Distillation. World Applied Science Journal, 7(4): pp.485-497
- Saad Mohsen Al-Mashat and Mohanad Ibrahim, 2017, Experimental Investigation of angle Basin Solar Still Coupled with Evacuated Tube Heat Pipe, Journal of Multi-disciplinary engineering Science and Technology (JMEST), Vol. 4 Issue 7.
- Sampath kumar K., Arjunan T. V. & Senthilkumar P., 2013, The Experimental Investigation of a Solar Still Coupled with an Evacuated Tube Collector, Energy Sources, Part A: Recovery, Utilization, and Environmental Effects, Volume 35, - Issue 3.
- Sampathkumar, K., Arjunan T.V. and Senthilkumar, P., 2011, Single Basin Solar Still Coupled with Evacuated Tubes - Thermal Modeling and Experimental Validation", International Energy Journal, Vol.12, pp.53-66.
- Tiwari G.N. and A.K., 2005, Effect of condensing cover's slope on internal heat and mass transfer in distillation: an indoor simulation Desalination, 180, pp.73-88.
- Tiwari, G.N., Dimri, V., Singh, U., Chel, A., and Sarkar, B., 2007, Comparative thermal performance evaluation of an active solar distillation system. International Journal of Energy Research 31: pp.1465-1482.
- Tiwari, G.N., Shukla S.K. and Singh I.P., 2003, Computer modeling of passive/active solar stills by using inner glass temperature. Desalination, 154, pp.171-185.
- Velmurugan V. and Srithar K., 2007, Solar stills integrated with a mini solar pond analytical simulation and experimental validation", Desalination; pp.216:232– 41.

NOMENCLATURE

Symbols	Description	Units	Symbols	Description	Units
Latin Symbols					
A	Area	m^2	L_b	Length of basin	m
B_b	Width of basin	m	$(MC)w$	Heat capacity of water mass in basin	$J/m^2.°C$
C_p	Specific heat	$J/kg.K^\circ$	m_{ew}	Hourly distillate yield	$kg/m^2.h$
$\frac{dT}{dt}$	Change in basin temperature in small time	$C°/s$	M_{ew}	Daily distillate yield	$kg/m^2.d$
$\frac{d_E}{dt}$	Rate change in in energy	J	M	Mass of water in the basin	kg
dt	Small time interval	Sec	P	Partial pressure	N/m^2
F	Form factor	-	Q	Heat flux	W/m^2
g	Gravitational constant	m/s^2	t	Time	Sec
G	Irradiance	W/m^2	Δt	Time interval	Sec

$G_{g,ef}$	Total effective irradiance on the water surface	W/m^2	ΔT	Difference between water and glass cover	$C°$
I_t	Insolation on passive solar still	W/m^2	U	Overall heat transfer coefficient	$W/m^2\ .k$
K	Thermal conductivity	$W/m\ .k$	V_w	Wind speed	m/s
LH_w	Latent heat of evaporation of water /condensation	J/kg	x_{gc}	Thickness of glass cover	m
$L\ ,Z$	Characteristic length	M	X	Thickness	m
Greek Symbols					
N	Kinematic viscosity	$m^2/\ s$	Σ	Summation	-
β'	Coefficient of thermal expansivity	$1/K$	α	Absorptivity	-
σ	Stefan-Boltzman coefficient	$W/m^2\ .K$	$\propto \tau$	absorptance – transmittance product	-
M	Dynamic viscosity	$kg/m\ .s$	Δ	Change in (Difference)	-
β	Angle of glass cover	degree	η_i	Instantaneous efficiency	-
τ	Transmissivity	-	ε	Emissivity	-
ε	Emisivity	-	ρ	Reflectance, density	-
Dimensionless Groups					
Bi	Biot number	-	Pr	Prandtl number	-
Gr	Grashof number	-	R_a	Rayleigh number	-
Nu	Nusslet number	-			
Subscript					
A	Air, ambient	-	gc	Glass cover	-
B	Basin-liner (Still basin plate)	-	**g, ef**	Global radiation on tilted surface	-
B	Beam	-	ins	Insulation	-
b-a	Basin liner to ambient	-	r	Radiative	-
bo	Bottom basin	-	sk	Sky	-
b-w	Basin liner to water	-	sw	side walls	-
C	Convective	-	t	Total	-
D	Diffuse	-	V	Vapor	-
E	Evaporative	-	W	Water	-
Eff	Effective	-	gc	Glass cover	-